Nonlinear surface lattice coupler

Xianling Shi,[1] Fangwei Ye,[1,*] Boris Malomed,[2] and Xianfeng Chen[1]

[1]*Department of Physics, Shanghai Jiao Tong University, Shanghai 200240, China*

[2]*Department of Physical Electronics, Faculty of Engineering, Tel Aviv University, Tel Aviv 69978, Israel*

**Corresponding author: fangweiye@sjtu.edu.cn*

Received December 18, 2012; accepted February 25, 2013;
posted February 28, 2013 (Doc. ID 181918); published March 21, 2013

We study two-component surface solitons in a pair of linearly coupled truncated waveguiding arrays with the Kerr nonlinearity. Symmetric solitons have a very small stability area, while those that are antisymmetric and asymmetric are stable in vast regions. Below a critical value of the coupling constant, branches of the symmetric and asymmetric modes separate, and accordingly, asymmetric solitons cease to bifurcate from the symmetric ones, providing the first example of asymmetric modes in nonlinear couplers that do not originate from symmetric counterparts. © 2013 Optical Society of America

OCIS codes: 190.0190, 190.6135.

Directional couplers, built of two parallel cores coupled by evanescent fields, are one of the basic elements in optical circuitry. If the Kerr coefficient is large enough, the energy exchange between the cores depends on the power [1], which gives rise to all-optical light switching [2–5]. Realizations of nonlinear couplers have been elaborated in many other settings, including semiconductor waveguides [4], twin-core Bragg gratings [6], plasmonic media [7], parallel arrays of discrete waveguides [8,9], cores with nonlocal nonlinearity [10], and nonlinear $\mathcal{PT}$-symmetric couplers [11,12].

The operation of a nonlinear directional coupler can be understood in terms of its symmetric, antisymmetric, and asymmetric supermodes. The asymmetric states have no counterparts in linear systems, appearing from the symmetric ones via a symmetry-breaking bifurcation (SBB) [3]. Further, the interplay of the intracore nonlinearity and temporal dispersion or spatial diffraction with the linear coupling gives rise to solitons, which also may be classified as symmetric, antisymmetric, and asymmetric. The instability of symmetric solitons [13] triggers the SBB of the subcritical [14] type (unlike the supercritical SBB of uniform states in the nonlinear coupler [3]). SBBs for solitons were studied in detail in the basic [15–17] and extended [6–12] models. In particular, the SBB keeps its subcritical character for two-component discrete solitons in discrete couplers [8].

Surface modes in semi-infinite waveguiding arrays have attracted a great deal of interest too, in theoretical [18–21] and experimental [22–25] studies alike. A natural setting, which is the subject of the present Letter, is the SBB and asymmetric surface solitons in a truncated dual-core array, see the inset in Fig. 1(a). Such a system can be readily created in experiments [22,23]. Using a systematic numerical analysis and the variational approximation (VA), we demonstrate that the surface strongly alters properties of asymmetric modes. In particular, a completely new feature is that, when the intercore coupling constant falls below a certain value, asymmetric modes do not bifurcate from symmetric ones, but exist as a disjoint family.

The light propagation along axis z in a pair of parallel-coupled semi-infinite waveguiding arrays is described by the following equations for field amplitudes u_n and v_n:

$$i\frac{du_n}{dz} = -\frac{1}{2}(u_{n+1} + u_{n-1} - 2u_n) - |u_n|^2 u_n - kv_n, \quad (1)$$

$$i\frac{dv_n}{dz} = -\frac{1}{2}(v_{n+1} + v_{n-1} - 2v_n) - |v_n|^2 v_n - ku_n, \quad (2)$$

at $n \geq 2$. At the edge ($n = 1$), we set $u_0 = v_0 = 0$ in the equations. Here the intersite coupling and self-focusing

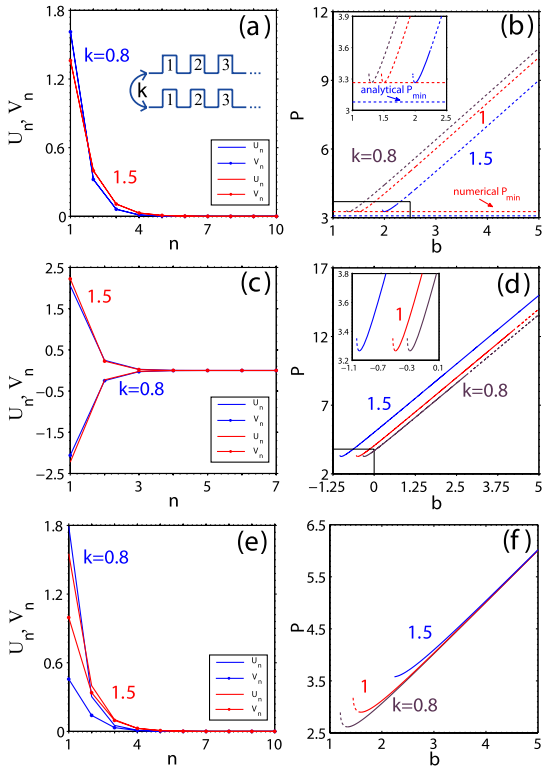

Fig. 1. (Color online) (a), (c), and (e), profiles of three types of surface solitons, *viz.*, symmetric (unstable), antisymmetric (stable), and symmetric (stable), respectively, for $b = 2.5$ and two different values of the coupling constant, $k = 0.8$ and 1.5. The inset in (a) is a sketch of the present system. Total power P is shown as a function of propagation constant b for the same three types in panels (b), (d), and (f), respectively. Insets in (b) and (d) zoom the boxed areas. Stable and unstable branches are plotted by solid and dashed curves, respectively. "Analytical" $P_{\min}$ in (b) is the value predicted by VA.

coefficients are scaled to be 1, while k accounts for the coupling between the arrays.

Stationary solutions with real propagation constant b are looked for as $\{u_n, v_n\} = \{U_n, V_n\}\exp(ibz)$ with real amplitude profiles U_n, V_n. We address fundamental discrete solitons pinned to the surface, i.e., with $|U_n|$ and $|V_n|$ attaining a maximum at $n = 1$ (solitons with the maximum shifted from the surface are possible too [20]). Representative examples of numerically found symmetric ($U_n = V_n$), antisymmetric ($U_n = -V_n$), and asymmetric ($|U_n| \neq |V_n|$) surface modes are shown in the left column of Fig. 1.

Properties of the discrete solitons are summarized in Figs. 1(b), 1(d), 1(f) and Fig. 2. The total power, $P = P_u + P_v \equiv \sum_{n=1}^{\infty}(U_n^2 + V_n^2)$, is plotted versus b in the right column of Fig. 1. All branches feature a minimum power $P_{\min}$, which is a typical feature of surface solitons [18–21], in contrast to discrete solitons in infinite lattices [14]. The quick termination of the power curves to the left of $P = P_{\min}$ is explained by abrupt growth of P due to delocalization of the solitons. The U-shaped $P(b)$ curves for symmetric and antisymmetric solitons differ solely by a horizontal shift, as their power depends on combination $(b \mp k)$, hence they share a common threshold, $P_{\min} = 3.2655$. The situation is different for asymmetric solitons, whose $P(b)$ curve significantly depends on k [Fig. 1(f)]. Their threshold power increases with k, and at $k > 1.5$ the negative-slope branch of the power curve disappears, leaving $P(b)$ a monotonously increasing function.

The family of asymmetric solitons is quantified in Fig. 2 by the asymmetry measure $\Theta = (P_v - P_u)/P$. Two top curves show that the asymmetric solitons emerge from symmetric ones via a subcritical SBB at $1.1 < k < 1.5$, which switches into a supercritical bifurcation at $k > 1.5$. The switch between the two different types of the SBB occurs in other models too; in particular, it follows the transition from the uniform coupling to that at a single site [9].

The most interesting finding demonstrated by Fig. 2 is that the asymmetric family completely separates from the symmetric one at $k < k_{\rm cr} \approx 1.1$. In this case, the asymmetric discrete solitons exist at Θ exceeding a certain minimum value, hence they cannot bifurcate from symmetric modes. This feature, which has no counterpart in previously studied nonlinear couplers, is the main result of this Letter. It is explained by the fact that, at $k = k_{\rm cr}$, the SBB happens exactly at $P = P_{\min}$, i.e., the SBB coincides with the saddle-node bifurcation that is responsible for the U-shape of the $P(b)$ curve for the symmetric solitons, and at $k < k_{\rm cr}$ the U-shaped power curves for the symmetric and asymmetric modes separate. The memory of the overlap of the two bifurcations at $k = k_{\rm cr}$ makes the symmetric-soliton family completely unstable at $k < k_{\rm cr}$.

The stability of the soliton families was tested by simulations of the perturbed evolution. Stable and unstable branches are indicated in Figs. 1 and 2 by solid and dashed lines, respectively. The result is that all the branches with $dP/db < 0$ are unstable, while the asymmetric solitons are always stable at $dP/db > 0$, in accordance with the Vakhitov–Kolokolov (VK) criterion [14]. Antisymmetric solitons are chiefly stable at $dP/db > 0$ [oscillatory destabilization of the branch with $k = 1.5$ at large values of b, observed in Fig. 1(d), cannot be detected by the VK criterion]. The symmetric solitons are stable at $dP/dk > 0$ (if the above-mentioned separation of the symmetric and asymmetric branches does not happen) prior to the SBB. As seen in Fig. 1(b), this condition is met only for a small part of the $P(k)$ curve at $b = 1.5$.

A typical example of the unstable propagation of symmetric solitons (Fig. 3) demonstrates that, as expected, unstable symmetric solitons quickly transform into an asymmetric stable mode, losing almost no power. Simulations of the propagation of unstable asymmetric solitons, which belong to the portion of the respective power curve with $dP/dk < 0$ (not shown here in detail) demonstrate that they transform into approximately symmetric delocalized modes, which extend into the depth of the lattice.

Numerical results presented above can be explained by a VA. Following [26], we adopt the ansatz for the stationary solution as $\{U_n, V_n\} = \{A, B\}\exp(-an)$, with respective powers $\{P_u, P_v\} = (1 - e^{-2a})^{-1}\{A^2, B^2\}$. The substitution of this into the Lagrangian of the stationary version of Eqs. (1) and (2) yields $L = (1/2)(b + 1 - e^{-a})(P_u + P_v) - k\sqrt{P_u P_v} - (1/4)(\tanh a)(P_u^2 + P_v^2)$, from

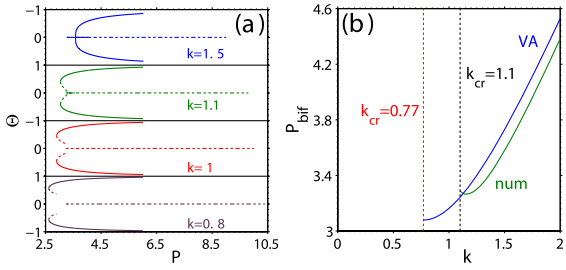

Fig. 2. (Color online) (a) Dependence of asymmetry measure Θ on the soliton's power at different values of k. (b) Power at which asymmetric solitons bifurcate from asymmetric ones, as predicted by the VA and found in the numerical form.

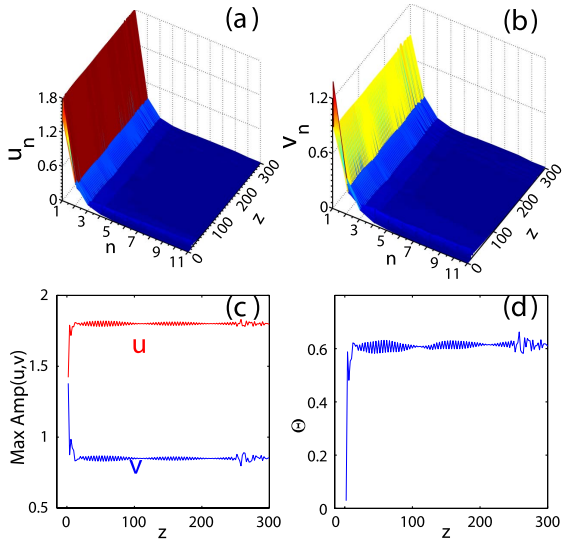

Fig. 3. (Color online) (a), (b), evolution of two components of an unstable symmetric soliton at $k = 1.5$, $b = 2.6$. (c), (d), the corresponding evolution of amplitudes of the two components and the soliton's asymmetry.

which the corresponding Euler–Lagrange equations follow, $\partial L/\partial P_{u,v} = \partial L/\partial a = 0$. Analysis of these equations for the symmetric solitons demonstrates that the VA correctly predicts the U-shape of the $P(b)$ curves, with the minimum power $P_{\min}^{(\mathrm{VA})} = 16/(3\sqrt{3}) \approx 3.08$, which differs by 5.7% from its numerical counterpart, see Fig. 1(b).

Further, the SBB point can be predicted by considering a solution to the variational equations with an infinitely small $(P_u - P_v)$. This condition leads to a system of equations for the power and inverse width of the soliton at the SBB: $P_{\mathrm{bif}} = k \coth a_{\mathrm{bif}}$, $\sinh(2a_{\mathrm{bif}}) = k \exp(a_{\mathrm{bif}})$. A numerical solution of the system yields a curve $P_{\mathrm{bif}}(k)$ displayed in Fig. 2(b). Although it starts at value $k_{\mathrm{cr}}^{(\mathrm{VA})} = 4/(3\sqrt{3}) \approx 0.77$, which is significantly smaller than its numerically found counterpart, $k_{\mathrm{cr}} \approx 1.1$ (the discrepancy is a consequence of inaccuracy of the ansatz at the critical point), the predicted dependence $P_{\mathrm{bif}}(k)$ is quite close to the numerical one at $k > 1.1$.

In conclusion, we have studied the influence of the surface on symmetric, antisymmetric, and asymmetric solitons in the truncated nonlinear lattice coupler. The noteworthy finding is the separation of the symmetric and asymmetric branches below the critical value of the coupling constant. In that case, the asymmetric solitons do not bifurcate from the symmetric ones, but exist as disconnected stable modes. This feature was not found in previously studied couplers.

F.Y. acknowledges support from NNSFC (No. 11104181), and from the Innovation Program of Shanghai Municipal Education Commission (No. 13ZZ022). F.Y. and B.M. appreciate hospitality of ICFO (Barcelona, Spain).

References

1. S. Jensen, IEEE J. Quantum Electron. **18**, 1580 (1982).
2. S. R. Friberg, Y. Silberberg, M. K. Oliver, M. J. Andrejco, M. A. Saifi, and P. W. Smith, Appl. Phys. Lett. **51**, 1135 (1987).
3. A. W. Snyder, D. J. Mitchell, L. Poladian, D. R. Rowland, and Y. Chen, J. Opt. Soc. Am. B **8**, 2102 (1991).
4. A. Villeneuve, C. C. Yang, P. C. J. Wigley, G. I. Stegeman, J. S. Aitchison, and C. N. Ironside, Appl. Phys. Lett. **61**, 147 (1992).
5. F. Lederer, G. I. Stegeman, D. N. Christodoulides, G. Assanto, M. Segev, and Y. Silberberg, Phys. Rep. **463**, 1 (2008).
6. W. C. K. Mak, B. A. Malomed, and P. L. Chu, J. Opt. Soc. Am. B **15**, 1685 (1998).
7. M. Hochberg, T. Baehr-Jones, C. Walker, and A. Scherer, Opt. Express **12**, 5481 (2004).
8. G. Herring, P. G. Kevrekidis, B. A. Malomed, R. Carretero-González, and D. J. Frantzeskakis, Phys. Rev. E **76**, 066606 (2007).
9. Lj. Hadžievski, G. Gligorić, A. Maluckov, and B. A. Malomed, Phys. Rev. A **82**, 033806 (2010).
10. X. Shi, B. A. Malomed, F. Ye, and X. Chen, Phys. Rev. A **85**, 053839 (2012).
11. R. Driben and B. A. Malomed, Opt. Lett. **36**, 4323 (2011).
12. N. V. Alexeeva, I. V. Barashenkov, A. A. Sukhorukov, and Y. S. Kivshar, Phys. Rev. A **85**, 063837 (2012).
13. E. M. Wright, G. I. Stegeman, and S. Wabnitz, Phys. Rev. A **40**, 4455 (1989).
14. P. G. Kevrekidis, *The Discrete Nonlinear Schrödinger Equation: Mathematical Analysis, Numerical Computations, and Physical Perspectives* (Springer, 2009).
15. C. Paré and M. Florjańczyk, Phys. Rev. A **41**, 6287 (1990).
16. A. I. Maimistov, Sov. J. Quantum Electron. **21**, 687 (1991).
17. M. Romagnoli, S. Trillo, and S. Wabnitz, Opt. Quantum Electron. **24**, S1237 (1992).
18. K. G. Makris, S. Suntsov, D. N. Christodoulides, G. I. Stegeman, and A. Hache, Opt. Lett. **30**, 2466 (2005).
19. Y. V. Kartashov, V. A. Vysloukh, and L. Torner, Phys. Rev. Lett. **96**, 073901 (2006).
20. M. I. Molina, R. A. Vicencio, and Y. S. Kivshar, Opt. Lett. **31**, 1693 (2006).
21. K. G. Makris, J. Hudock, D. N. Christodoulides, G. I. Stegeman, O. Manela, and M. Segev, Opt. Lett. **31**, 2774 (2006).
22. S. Suntsov, K. G. Makris, D. N. Christodoulides, G. I. Stegeman, A. Hache, R. Morandotti, H. Yang, G. Salamo, and M. Sorel, Phys. Rev. Lett. **96**, 063901 (2006).
23. E. Smirnov, M. Stepić, C. E. Rüter, D. Kip, and V. Shandarov, Opt. Lett. **31**, 2338 (2006).
24. X. S. Wang, A. Bezryadina, Z. G. Chen, K. G. Makris, D. N. Christodoulides, and G. I. Stegeman, Phys. Rev. Lett. **98**, 123903 (2007).
25. A. Szameit, Y. V. Kartashov, F. Dreisow, T. Pertsch, S. Nolte, A. Tünnermann, and L. Torner, Phys. Rev. Lett. **98**, 173903 (2007).
26. B. A. Malomed, D. J. Kaup, and R. A. Van Gorder, Phys. Rev. E **85**, 026604 (2012).